THE ASTROPHYSICAL JOURNAL, 471:726–736, 1996 November 10

SYNTHESIS OF STELLAR Mg AND Fe ABSORPTION INDICES FOR STELLAR POPULATION STUDIES. II. THE EXTENDED AND UP-TO-DATE COLLECTION

M. CHAVEZ
Instituto Nacional de Astrofisica, Optica y Electronica, Apdos. Postales 51 y 216, 72000 Puebla, Pue., Mexico[1]
M. L. MALAGNINI
Dipartimento di Astronomia, Università degli Studi di Trieste, via Tiepolo 11, I-34131 Trieste, Italy
AND
C. MOROSSI
Osservatorio Astronomico di Trieste, via Tiepolo 11, I-34131 Trieste, Italy
Received 1996 January 9; accepted 1996 June 3

ABSTRACT

This paper is mainly concerned with the prediction of absorption-line spectral features in cool stars, to be used as input in stellar population synthesis projects. From a detailed comparison with the solar intensity spectrum, we have refined the main parameters of atomic and molecular absorption lines that are prominent in the 4850–5400 Å wavelength interval. This line list was used to compute an extensive library of synthetic stellar spectra at high resolution in the temperature range $T_{\rm eff} = 4000$–8000 K, surface gravity interval $\log g = 1.0$–5.0 dex, metallicities ([M/H]) from -1.0 to $+0.5$ dex, and microturbulent velocity $\xi = 2$ km s^{-1}. The computations were performed by using the latest release of Kurucz's model atmospheres and numerical codes. The library contains a total of 693 synthetic spectra, from which iron and magnesium indices were obtained, together with the corresponding "pseudocontinuum" fluxes.

We illustrate the behavior of five "Lick-like" spectral indices, namely, Mg_1, Mg_2, Mg b, Fe5270, and Fe5335, in terms of the main atmospheric parameters, namely, effective temperature, surface gravity, and metallicity. The trend of the indices with microturbulent velocity is also illustrated by means of an additional set of spectra computed at different microturbulent velocities. Transformation equations of the theoretical grid into the Lick/IDS observational database are presented, showing the full consistency of our grid with the empirical database.

Subject heading: galaxies: stellar content — stars: atmospheres — stars: late-type

1. INTRODUCTION

The study of prominent absorption features in galaxies is a fundamental step toward understanding the chemical history of their stellar populations. Before using spectral indices in the study of stellar populations, it is mandatory to investigate and determine the relationships between features and stellar atmospheric parameters. These investigations have been carried out empirically from the analysis of observed spectra (e.g., Faber et al. 1985; Buzzoni, Gariboldi, & Mantegazza 1992; Gorgas et al. 1993; Worthey et al. 1994, hereafter WFGB94; Buzzoni, Mantegazza, & Gariboldi 1994; Borges et al. 1995) and theoretically, by computing synthetic spectra (e.g., Mould 1978; Barbuy 1989, 1994; Gulati, Malagnini, & Morossi 1991, 1993; McQuitty et al. 1994; Chavez, Malagnini, & Morossi 1995; Tripicco & Bell 1995).

Among the empirical libraries of stellar spectra and collections of indices, the most extensive is that created by S. Faber and coworkers at Lick Observatory (see WFGB94 and references therein). The Lick/IDS database contains ~460 stellar spectra in the 4000–6400 Å region and includes the material presented by Faber et al. (1985) and Gorgas et al. (1993). The resolution of the spectra is estimated to be 8.2 Å. The database collection of 21 absorption spectral indices constitutes the Lick/IDS system. The indices are calibrated through polynomial fitting functions, yielding the relationships between each index and the set of stellar atmospheric parameters. The parameters assigned to each star are obtained from the literature or derived from observed quantities (e.g., $V-K$ is used to derive effective temperature).

Buzzoni et al. (1992) carried out a quantitative calibration of the Mg_2 index by deriving the trend of the index as a function of stellar atmospheric parameters. Their stellar database, after normalization to the Lick/IDS system, was applied to population synthesis for studying the effects on the integrated indices of simple stellar populations due to changes either in the initial mass function or in age or metallicity. Their analysis was later expanded to iron and Hβ indices (Buzzoni et al. 1994).

On the theoretical side (see references above), synthetic spectra are used instead of the observed ones to fill the gaps in poorly observed stellar evolutionary stages. In fact, synthetic spectra can be computed for almost any combination of atmospheric parameters and, moreover, can be unambiguously labeled in terms of atmospheric parameters from the parent model. These characteristics differentiate the theoretical approach from the empirical one since, in the latter, the parameters assigned to each star are in general neither unique nor homogeneously derived.

[1] Also Scuola Internazionale Superiore di Studi Avanzati (SISSA/ISAS), Trieste, Italy.

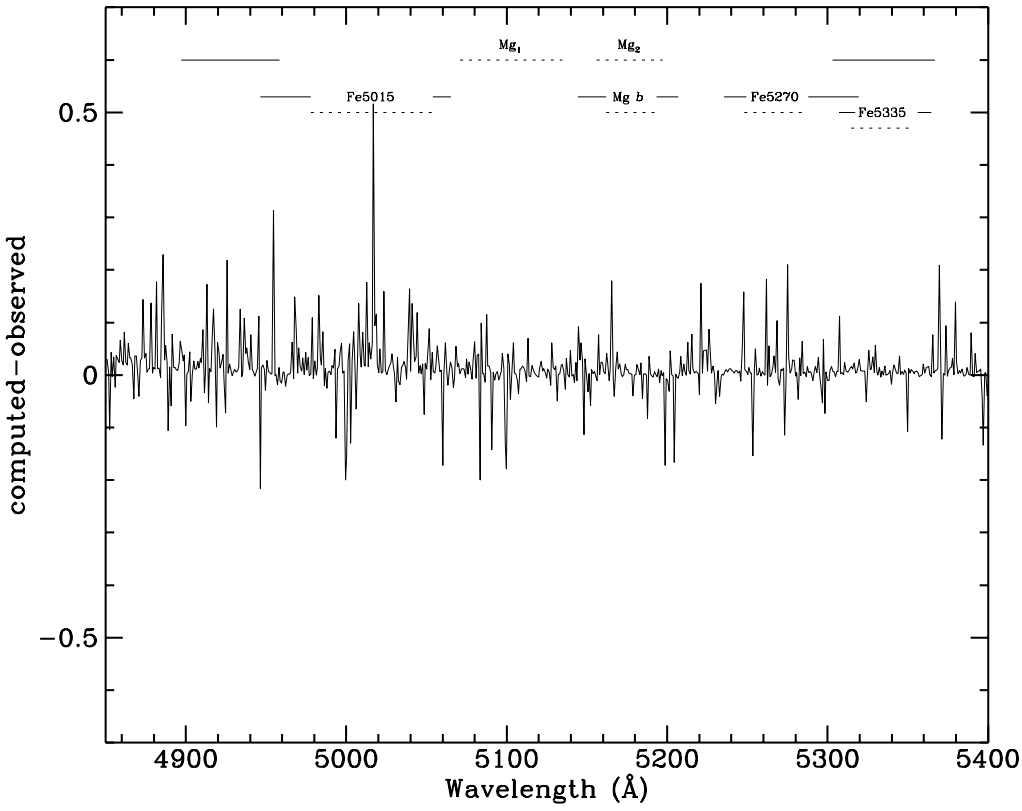

FIG. 1.—Differences between computed and observed normalized solar spectra after revising the original Kurucz input line-list parameters. The largest positive residuals appear in the region where the index Fe5015 is defined.

In a recent paper, Tripicco & Bell (1995) exploited the possibility of modeling the Lick/IDS spectral indices by use of synthetic spectra: they used the MARCS (Gustafsson et al. 1975) and SSG (Bell & Gustafsson 1978, 1989; Gustafsson & Bell 1979) codes. They calculated synthetic spectral indices for temperature and gravity along a 5 Gyr isochrone and found "generally good agreement" with the observed indices of M67 and field stars.

This paper proceeds on the line of work carried out in Trieste (see Chavez et al. 1995 and references therein) and provides an updated and extended grid of synthetic indices based on new input data and codes.

We stress that the indices of our grid, like those computed by Tripicco & Bell (1995), are purely theoretical. The main difference between the two collections lies in the fact that our indices are uncalibrated, and therefore they need a suitable calibration before any comparison with observational data. In this paper, we illustrate for example how our grid can be transformed into the Lick/IDS system.

To build, in a self-consistent way (as discussed in the Appendix), the synthetic integrated index of a stellar system from our indices, which refer to single stellar components, our index collection is supplemented by the proper "pseudocontinuum" fluxes.

In § 2, we present some details of the comparison between theoretical and observed solar spectra. In § 3, we describe the characteristics of the library of synthetic spectra, while the calculation of spectral indices and their dependence on key atmospheric parameters are presented in § 4. Section 5 is devoted to the comparison between the grid of indices and the Lick/IDS stellar database. We summarize and draw conclusions in § 6.

2. THE SOLAR SPECTRUM: ADJUSTMENT OF LINE PARAMETERS

One of the most important ingredients needed in the computation of theoretical spectra is the absorption-line data to be considered in the spectral interval of interest. Thus, prior to the computation of a synthetic spectrum, there is one important factor to be taken into account, i.e., the limited accuracy of the agents that affect the line profile and strength, as pointed out by Kurucz (1995). In order to increase the accuracy of these agents, we have compared a theoretical solar spectrum with the solar central intensity spectrum observed by J. Brault, as reduced and digitized by Kurucz (1991). The aim of this comparison is twofold: first, to improve the line parameters and, second, to identify spectral regions where the match is not satisfactory and where the reliability of the theoretical spectral indices there defined will be doubtful.

The lines to be included in our computations have been extracted from the most updated atomic and molecular line lists compiled by Kurucz and colleagues. The original lists contain information on nearly 58 million lines of atoms, up to the 10th stage of ionization, and of diatomic molecules. Over 45,000 lines in the 4850–5400 Å wavelength region have been taken into account for the comparison. Molecules considered in our computations are CN, C_2, MgH, SiH, and CH, which are responsible for the vast majority of the relevant lines.

The solar model used for the comparison has the following atmospheric parameters: $T_{\rm eff} = 5777$ K, $\log g = 4.43770$, and elemental abundances from Anders & Grevesse (1989). The adopted micro- and macroturbulent

velocity values are 1.0 and 1.5 km s^{-1}, respectively (see Thévenin 1989 and references therein). In order to match the resolution of the observed spectrum, the synthetic spectrum was computed with a resolving power of $\lambda/\Delta\lambda = 522{,}000$. A trial-and-error procedure (see, e.g., Peterson, Dalle Ore, & Kurucz 1993) was used to modify the line parameters and to compare the spectra until a satisfactory match was obtained.

We started by modifying the log *gf*–values of the strongest lines and then moved to the weakest ones. Regarding the damping constants, van der Waals pressure broadening is the dominant process in cool stars for nonhydrogen lines. As a consequence, van der Waals damping constants were modified, if necessary, to obtain a good representation of the line wings of the strongest lines.

In general, the match was considered satisfactory if the difference in the peak residual intensities between the observed and the theoretical lines was less than 0.05. A total of $\sim$2000 modifications were performed on the main parameters of some 1500 lines. In order to illustrate the importance of these corrections, in Figure 1 we show the differences—computed minus observed spectra (both normalized to the continuum)—after making the modifications to the line parameters. For the sake of clarity, the spectra were rebinned with a fixed wavelength step.

The standard deviation of the distribution of the differences, which was 0.09 before the fine-tuning of the line parameters, decreased to 0.06 by using the modified line list in the computation of the theoretical spectrum. This is mainly due to the disappearance of the negative residuals (below the -0.2 level), which corresponded to spectral lines in excess (or stronger) in the theoretical spectrum computed with the original line list. These residuals were effectively reduced by properly modifying the log *gf*–values of the proper lines. On the other side, positive residuals indicate lines that are weaker in the theoretical spectrum. Again, the residuals can be reduced by changing the log *gf*–values, but only if the observed line can be identified unambiguously. Unfortunately, this was sometimes impossible, and since no correction was attempted in these cases, large positive residuals (up to a $+0.5$ level) are still present in Figure 1.

3. SYNTHETIC SPECTRA

Based on the modified line list described above, we computed nearly 700 synthetic spectra from the subsample of Kurucz (1993a, 1993b, 1993c) model atmospheres, covering an effective temperature range between 4000 and 6000 K at a step of 250 K plus the spectra at 7000 and 8000 K, surface gravity from 1.0 to 5.0 dex at a step of 0.5 dex, and metallicities [M/H] $= -1.0, -0.5, 0.0, 0.1, 0.2, 0.3$, and 0.5.

The wavelength range and the temperature interval were fixed in such a way as to yield a coverage as complete as possible of the domain of the most popular and widely used Mg and Fe indices, namely, Mg_1, Mg_2, Mg *b*, Fe5015, Fe5270, and Fe5335. The temperature upper limit is such that the Mg and Fe features vanish for temperatures beyond this limit (see Figs. 2–6 and WFGB94); the lower limit is forced by the low reliability of theoretical models and poor knowledge of molecular line opacities below 4000 K (see Gustafsson & Jørgensen 1994). The main computational characteristics of the synthetic spectra are as in Chavez et al. (1995), i.e., microturbulent velocity $\xi = 2$ km s^{-1}, rotational velocity $v_{rot} = 0$ km s^{-1}, and resolving power $\lambda/\Delta\lambda = 250{,}000$.

We point out that we assumed solar ratios for the abundances of all elements. The deviations from solar-partition abundances in globular clusters is a widely debated topic (see, e.g., Kraft 1994 and references therein). In particular, not only may variations in the relative abundances [C/Fe], [N/Fe], and [O/Fe] due to evolutionary effects or to primordial inhomogeneities be important, but α-element enhancements with respect to solar values could also play a

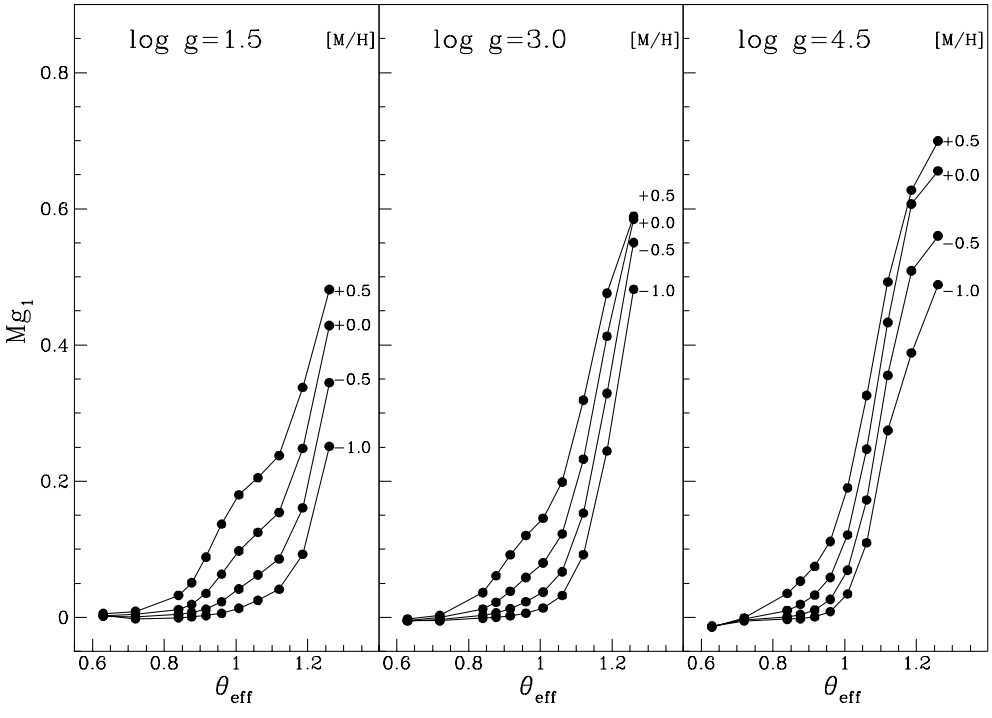

FIG. 2.—Mg_1 indices for different metallicities and gravities as a function of $\theta_{eff} = 5040/T_{eff}$

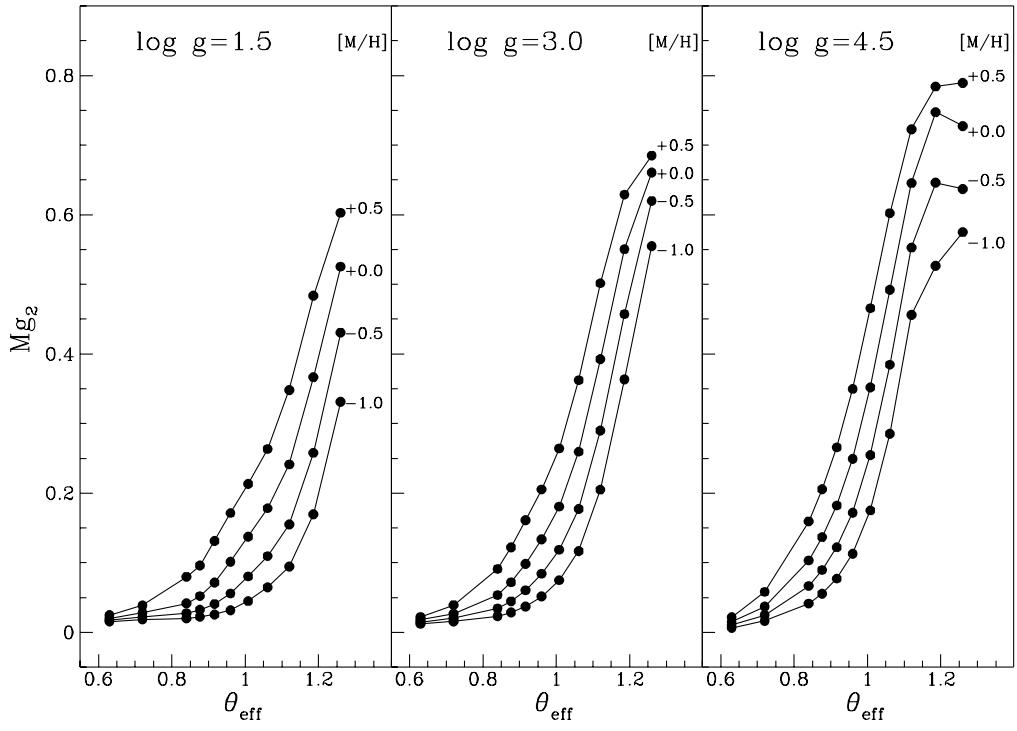

FIG. 3.—Same as Fig. 2, but for Mg_2

role in the interpretation of integrated spectra of stellar populations (in particular, for low-metallicity systems, i.e., [Fe/H] < -1; see Pagel 1996). Unfortunately, the complete investigation of this problem via computation of synthetic indices is hampered by the lack of ad hoc atmospheric models and opacities. As a consequence, we built a database under the assumption of scaled solar-partition abundances to constitute a reference point while we postponed addressing the nonsolar-partition problem, awaiting the announced new Kurucz models.

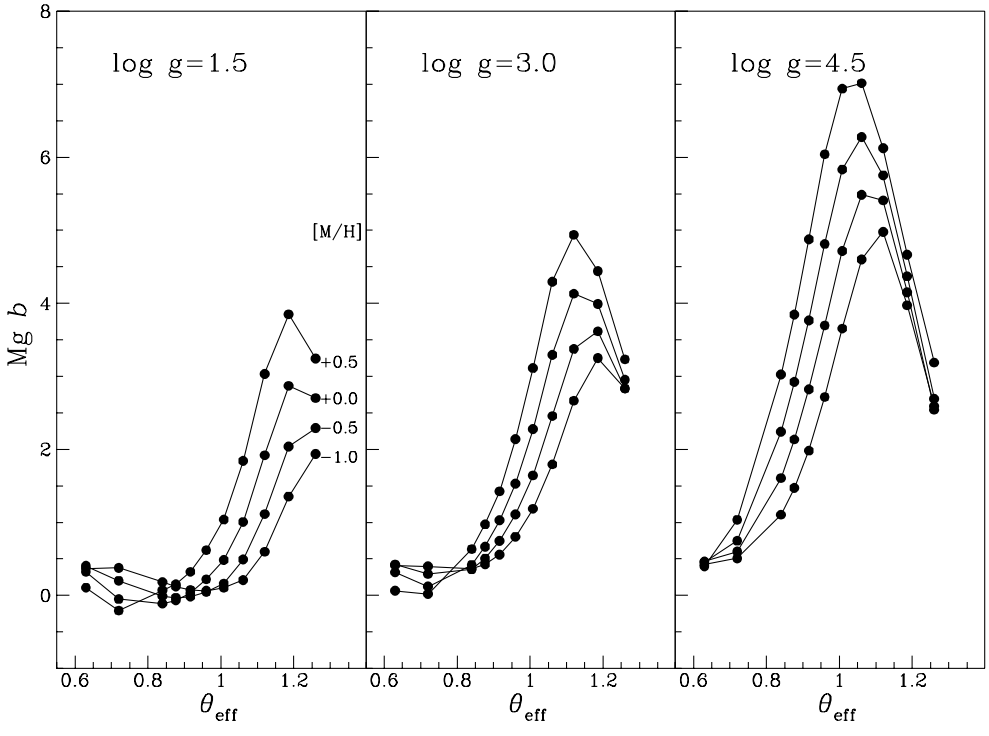

FIG. 4.—Same as Fig. 2, but for Mg *b*

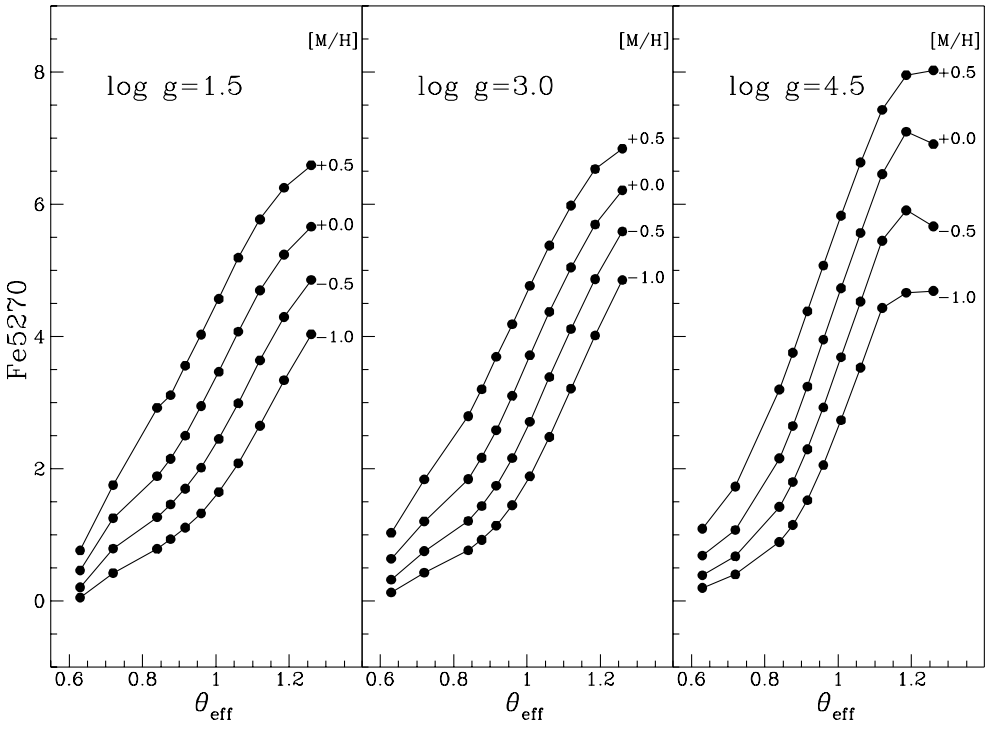

FIG. 5.—Same as Fig. 2, but for Fe5270

We have discussed in § 2 the importance of working on the atomic and molecular line list before using it to compute synthetic spectra. In order to obtain insight into the adequacy of the synthetic spectra for reproducing the observed features, we used as a fundamental check the results obtainable for the solar spectral indices. For the computation of indices, we have followed the definitions of Worthey (1992) and WFGB94 and used the revised values of the extrema of

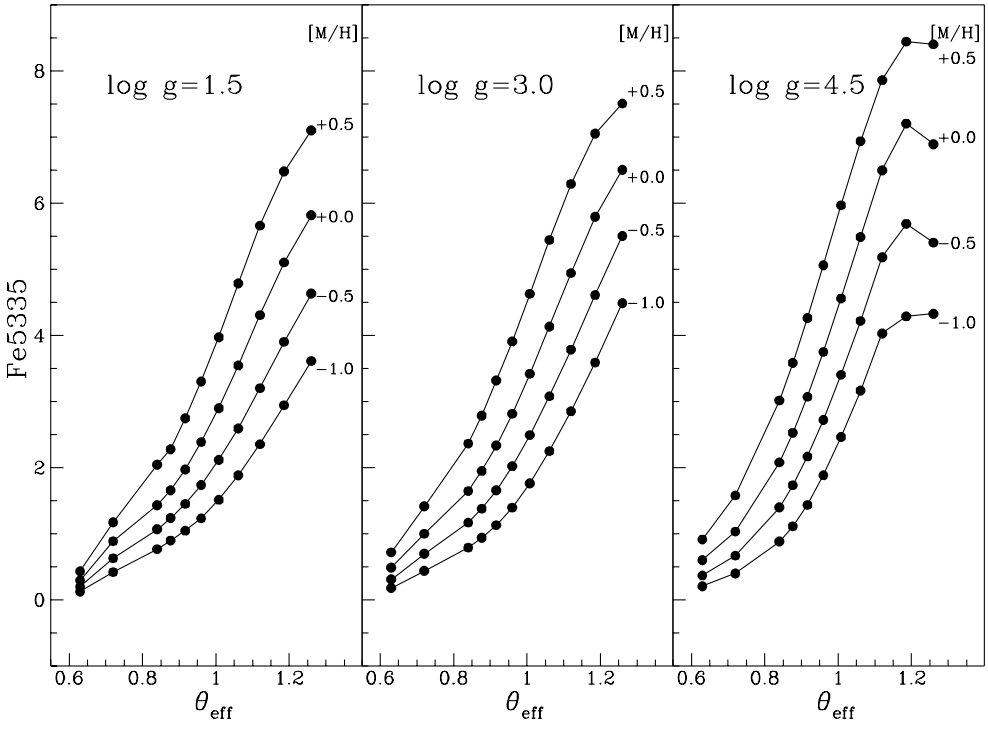

FIG. 6.—Same as Fig. 2, but for Fe5335

TABLE 1

SPECTRAL INDICES FOR THE SUN

Index (1)	Uncorrected (2)	Modified List (3)	Observed (4)	Δ(Index) (5)	rms[a] (6)
Mg_1	0.195	0.015	0.011	+0.004	0.007
Mg_2	0.146	0.130	0.124	+0.006	0.008
Mg *b*	3.445	3.017	3.061	−0.042	0.23
Fe5015.....	4.257	3.701	4.316	−0.615	0.46
Fe5270.....	2.625	2.356	2.485	−0.129	0.28
Fe5335.....	2.673	2.114	2.183	+0.069	0.26

[a] Typical rms error of stellar index observations as reported in Worthey et al. 1994.

the bands given in the latter reference. The wavelength interval covered by our library of synthetic spectra permits us to calculate six of the 21 indices listed in WFGB94.

3.1. *Spectral Indices for the Sun*

From the theoretical solar spectra, computed with and without adjustments to the line parameters, we computed the spectral indices listed in Table 1. Columns (2) and (3) show the indices obtained by using the line list before and after the corrections, respectively, while column (4) contains the indices computed from the observed solar spectrum. In column (5), we list the residuals obtained by subtracting from the theoretical indices (col. [3]) the observed values. As a term of comparison, column (6) contains the typical rms error of stellar index observations as reported in WFGB94.

The improvement obtained by using the modified line list is clear for all but one of the indices (i.e., Fe5015) from

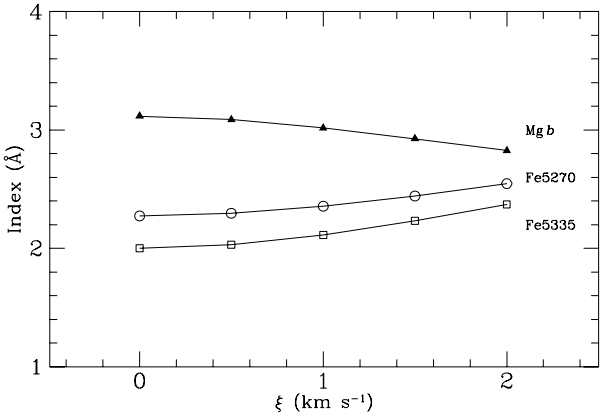

FIG. 7.—Equivalent widths of Mg *b*, Fe5270, and Fe5335 from the solar spectrum as a function of the microturbulent velocity ξ.

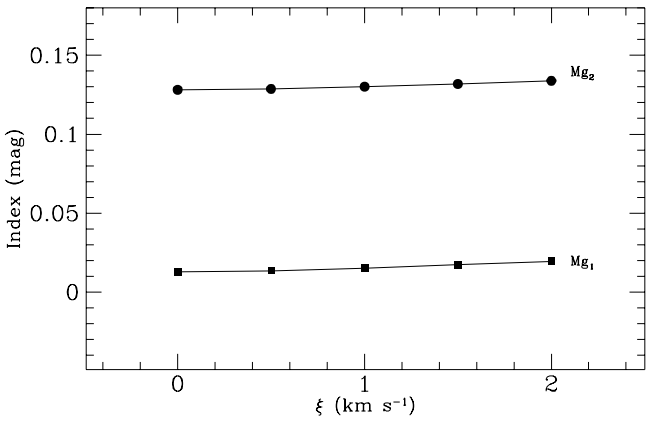

FIG. 8.—Same as Fig. 7, but for spectral indices Mg_1 and Mg_2

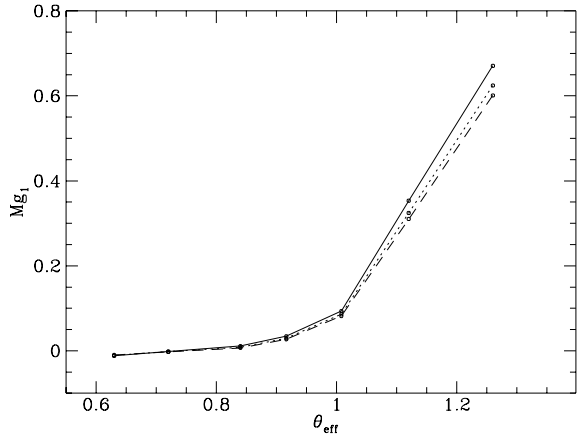

FIG. 9.—Spectral index Mg_1 for solar metallicity and log $g = 4.0$ as a function of θ_{eff} for different values of the microturbulent velocity ξ. The values of the index corresponding to $\xi = 0$, 1, and 2 km s^{-1} are connected by dashed, dotted, and solid lines, respectively.

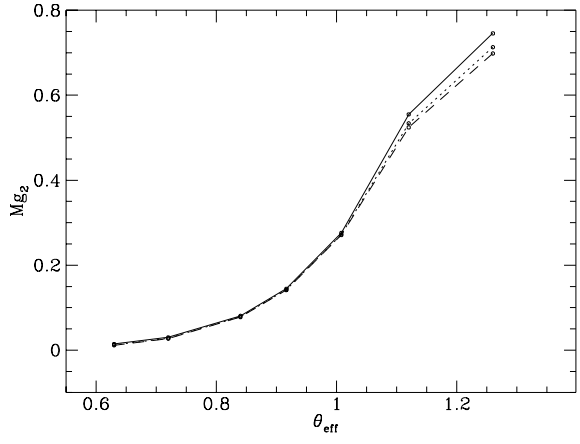

FIG. 10.—Same as Fig. 9, but for Mg_2

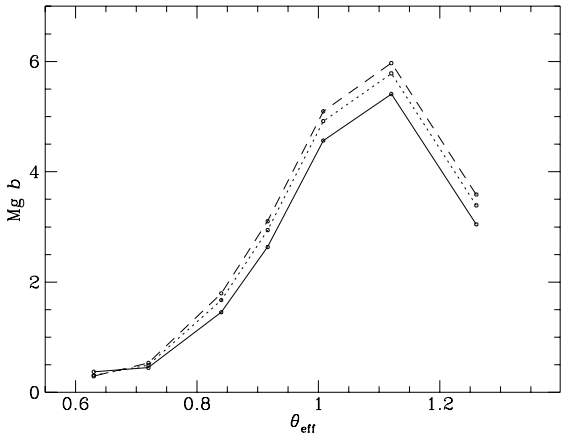

FIG. 11.—Same as Fig. 9, but for Mg *b*

comparison of columns (2) and (3). A comparison between columns (5) and (6) of Table 1 yields the following results: For Mg_1, Mg_2, and Fe5270, the residuals are about one-half of WFGB94's rms errors while, for Mg *b* and Fe5335, this figure is reduced to one-fourth. Regarding Fe5015, it appears that the index was in better agreement with the observed value before rather than after the line-list corrections. However, this agreement was actually fortuitous: Numerous lines in the wavelength region that defines the Fe5015 index were predicted in excess in the synthetic spectrum or, conversely, not accounted for, even if clearly present in the solar observed spectrum, thus roughly compensating each other. In the synthetic spectrum that was computed starting from the modified list, we zeroed all the features predicted but not observed, while we could not eliminate the problem of the observed but unidentified ones. The largest positive residual (0.5) shown in Figure 1 actually falls in the bandpass of Fe5015, thus implying a greater value of the theoretical index with respect to that observed (Table 1). It is interesting to note that Tripicco & Bell (1995) also found discrepancies in the case of this index between their predictions and observations, even though they did not find large discrepancies between computed and observed spectra. Our conclusion is that the reliability of the computed Fe5015 is, in any case, much lower than that of the other indices, and as a consequence we decided to exclude this index from further analysis.

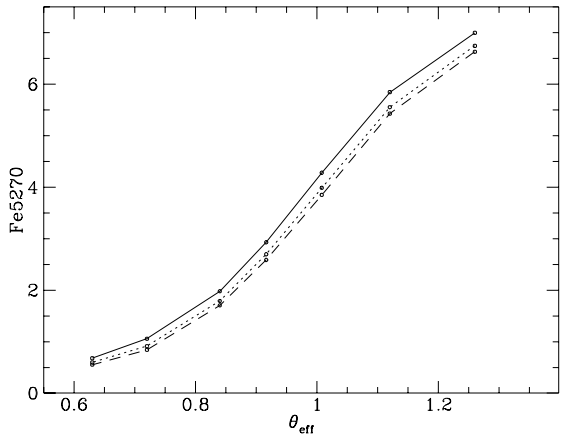

FIG. 12.—Same as Fig. 9, but for Fe5270

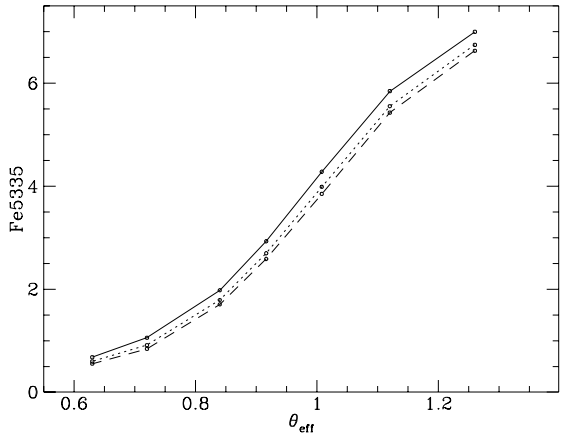

FIG. 13.—Same as Fig. 9, but for Fe5335

4. SPECTRAL INDICES AND ATMOSPHERIC PARAMETERS

In this section, the theoretical relationships between indices and stellar atmospheric parameters are illustrated with reference to a selected subset of parameters (the indices computed for the whole spectral library are presented in Chavez 1995 and in the CD-ROM produced as part of the proceedings of the meeting "From Stars to Galaxies: The Impact of Stellar Physics on Galaxy Evolution"; see Leitherer, Fritze–von Alvensleben, & Huchra 1996).

4.1. *Effective Temperature, Surface Gravity, and Overall Metallicity*

In Figures 2–6, we show the trend of each index with effective temperature for three surface gravities and four metallicities. Each figure contains three panels, in which we plot the index values versus the inverse effective temperature, $\theta_{\rm eff}$ ($\equiv 5040/T_{\rm eff}$). Each panel refers to one surface gravity value (1.5, 3.0, and 4.5 dex, respectively) and four different metallicities; circles represent the indices computed for 11 $T_{\rm eff}$-values from 4000 to 6000 K, at a step of 250 K, plus the indices for $T_{\rm eff} = 7000$ and 8000 K.

In general, the indices steeply increase with increasing $\theta_{\rm eff}$ until a maximum is achieved; then sometimes a decrease follows. At high temperatures, all indices tend to zero and some equivalent widths assume negative values, thus implying that the nominal feature is no longer prominent with respect to the corresponding "pseudocontinuum."

4.2. *Microturbulent Velocity*

We computed the library of synthetic spectra from model atmospheres all of which consider $\xi = 2$ km s^{-1}. In order to have some hint of the dependence of the indices on microturbulent velocity, we computed the solar indices by using synthetic spectra starting from models with $\xi = 0.0$, 0.5, 1.0, 1.5, and 2.0 km s^{-1}. The results for the indices measured as equivalent widths and for those measured in magnitudes are displayed in Figures 7 and 8, respectively.

From these figures, it is evident that all the indices but one, Mg *b*, increase with increasing microturbulent velocity. Assuming that the stellar ξ has an uncertainty of ± 1 km

s^{-1}, we expect that small corrections to the data presented here, at least for solar-like stars, may be required.

To obtain further insight into the influence of ξ, we computed a set of synthetic spectra and indices for dwarf stars ($\log g = 4.0$) at $\xi = 0.0$ and 1.0 km s^{-1} from Kurucz (1993c). The main results are shown in Figures 9–13. In all cases, the effect of ξ increases with decreasing temperature. For all the indices but Mg *b*, a decrease of 1 km s^{-1} in ξ may mimic a decrease in metallicity of $\sim$0.25 dex at most; on the contrary, a larger (0.5 dex) and opposite effect is shown by Mg *b*.

5. COMPARISON WITH THE LICK/IDS DATABASE

Our grid of indices does not necessarily reproduce any observational system but, rather, must be calibrated to be compared with any observational set. In this section, we present, as an example, a comparison between our indices and the most homogeneous collection of measured indices, presented by the Lick group (WFGB94) and kindly made available to us in computer-readable form by its authors. It is important to note that these indices were computed directly from spectra given in counts per pixel and divided by the response of a quartz lamp, thus affecting the overall spectral shape (S. M. Faber 1994, private communication), while our grid of indices was computed from theoretical, absolutely calibrated fluxes. We also bear in mind that the wavelength scale of the Lick/IDS spectra may potentially be off by 1–2 Å.

Tripicco & Bell (1995) adopted the following approach to the problem of transforming synthetic indices into the observational system: Their computed spectra were modified to mimic the Lick/IDS spectral response by using as template a number of IDS spectra made available to them by G. Worthey. From the transformed spectra, they derived synthetic indices directly comparable with those listed in WFGB94.

Since we started from a grid of theoretical indices, we adopted a different approach. We decided to derive direct transformation equations between our synthetic indices and the Lick/IDS ones. We compared theoretical and observed indices for as many stars as possible in order to compute zero points and scaling factors. We selected all HD stars whose atmospheric parameters ($T_{\rm eff}$, $\log g$, [Fe/H]), as given in the WFGB94 catalog, fell within the boundaries of our theoretical grid. Actually, these atmospheric parameters were used to obtain synthetic uncalibrated-calibrated indices from our grid, by interpolating linearly in the three-dimensional space ($T_{\rm eff}$, $\log g$, [M/H]). Recall that, since in the models all the metal abundances are scaled by the same factor with respect to the solar ones, we assumed that the observed [Fe/H]'s correspond to the theoretical [M/H]'s.

In order to derive the transformation equations, we computed a linear least-squares fit of the observed versus synthetic indices. The data for the 168 stars extracted from the catalog were considered to be 168 independent points, and the interactive NFIT1D STSDAS (1993) task was used to compute the zero points and scaling factors for each index; several iterations were performed, adopting a 3 σ threshold, to reject the outliers (see Figs. 14–18). Table 2 shows the results of the fittings: the number of points, the root mean square error of the fit ("rmse"), the zero point, and the scale factor, for each index.

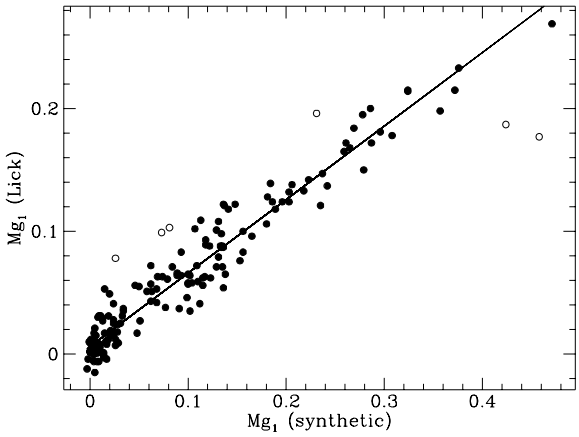

FIG. 14.—Calibration of the Mg_1 index. The abscissas represent the synthetic index, and the ordinates represent the observed Lick/IDS index. The least-squares fit is indicated by the solid line; open circles denote rejected points.

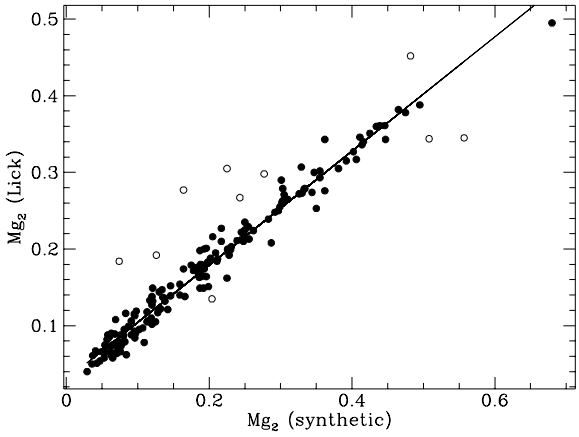

FIG. 15.—Same as Fig. 14, but for Mg_2

TABLE 2

CALIBRATION OF SYNTHETIC INDICES

			Zero Point		Scale Factor	
Index	Number of Points	rmse[a]	C_1	ΔC_1	C_2	ΔC_2
Mg_1.....	160	0.015	0.006	0.002	0.598	0.012
Mg_2.....	158	0.015	0.030	0.002	0.745	0.010
Mg *b*.....	166	0.513	0.582	0.094	0.949	0.031
Fe5270.....	161	0.288	0.129	0.070	0.720	0.017
Fe5335.....	164	0.298	0.017	0.067	0.671	0.018

[a] Root mean square error of the fit.

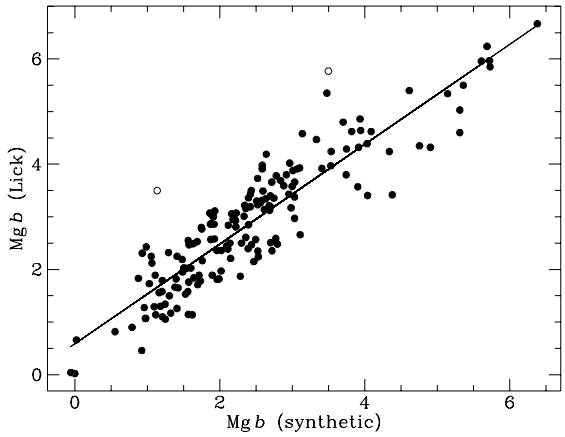

FIG. 16.—Same as Fig. 14, but for Mg *b*

The range of validity of the proposed transformation equations can be inferred from the distributions of the 168 stars in $T_{\rm eff}$, log *g*, and [Fe/H]. Figures 19 and 20 show that both temperature and gravity have bimodal distributions, with peaks at 4750 and 5750 K and at 2.25 and 4.25 dex, respectively. Figure 21 shows that most stars have metallicities in the interval from -0.5 to $+0.4$ dex while very few stars have lower metallicities.

As can be seen by comparing column (6) of Table 1 to the third column of Table 2, the rmse's are of the same order as

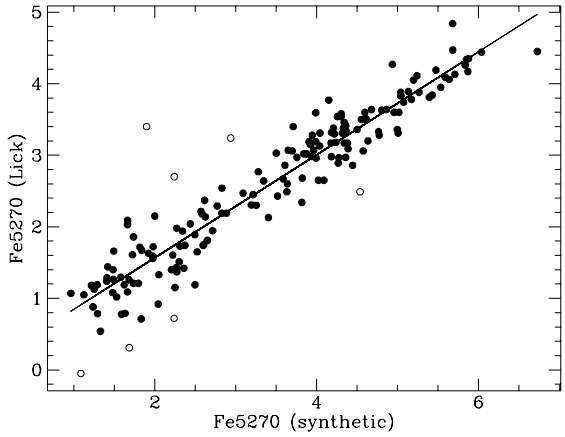

FIG. 17.—Same as Fig. 14, but for Fe5270

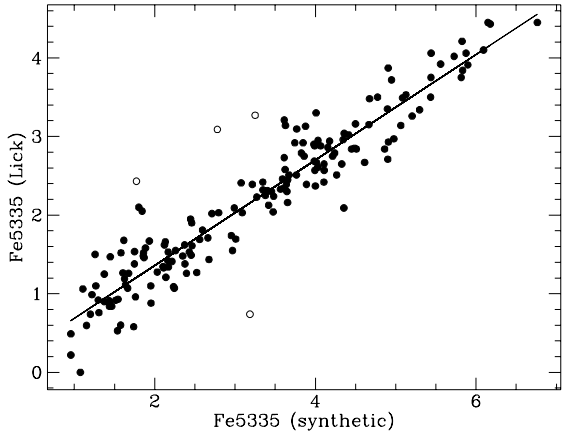

FIG. 18.—Same as Fig. 14, but for Fe5335

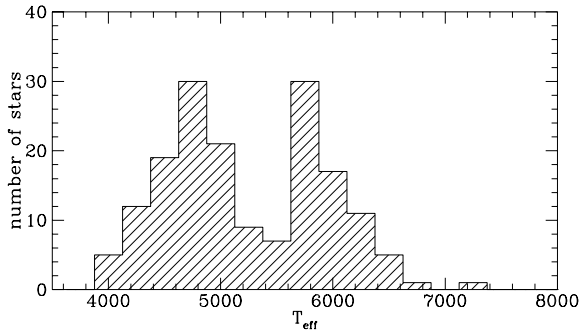

FIG. 19.—Histogram of temperatures of the stars used to transform the synthetic grid into the Lick/IDS system.

the observational errors for the Mg *b*, Fe5270, and Fe5335 indices, thus confirming the goodness of the fit. The fit is also quite good for Mg_1 and Mg_2, but the rmse values for these two indices are roughly twice the WFGB94 errors. This fact can be attributed to the high sensitivity of these indices to the atmospheric parameters. As a consequence, any error in the adopted stellar parameters will be reflected as an increase of the scatter in the plots of observed versus synthetic indices (see, for the case of Mg_2, the more detailed discussion in Chavez et al. 1995), thus producing higher than expected rmse's. The same kind of problem may be invoked to explain the outliers rejected in the fitting procedure. Very likely, the WFGB94 atmospheric parameters of these stars are too far from the correct values and produce synthetic indices very far from those observed. A further confirmation of this hypothesis comes from the fact that the indices of these stars correspond, in general, to outliers in more than one of Figures 14–18.

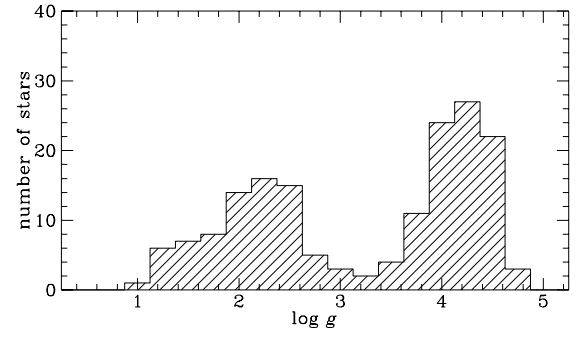

FIG. 20.—Same as Fig. 19, but for the gravities used

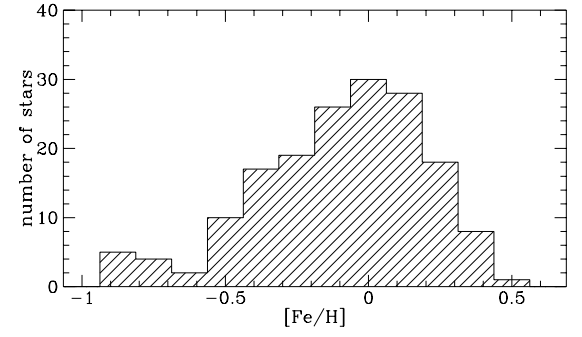

FIG. 21.—Same as Fig. 19, but for the metallicities [Fe/H] used

The fact that there is no need to introduce into the transformation equation any term but the zero points and the scaling factors clearly indicates that there is full consistency between our synthetic indices and the Lick/IDS database, thus stressing the validity of our grid.

6. SUMMARY AND CONCLUDING REMARKS

The grid presented here is, to our knowledge, the most comprehensive ever computed at high resolution. There are multiple applications of the synthetic indices described above. First, in the context of stellar populations, they provide a very attractive and self-consistent (see Appendix) alternative to the use of empirical calibrations in the derivation of integrated indices. We stress that, by using synthetic indices, we have the automatic correspondence of indices and stellar atmospheric parameters and therefore that a detailed description of the indices' behavior in terms of the atmospheric parameters is straightforward. Moreover, no commixture of empirical and theoretical data is needed, because of the availability of both features and "pseudocontinuum" fluxes.

The fact that the indices are computed without assuming any instrumental response or resolution makes it easy to match, after proper calibration, any high- or low-resolution observations, as shown for the case of the Lick/IDS database. Thus our grid of indices is a valuable tool for

Deriving stellar atmospheric parameters (often ill-determined) through comparison with indices of individual stars obtained at quite high resolution; and

Computing integrated indices for population synthesis studies of clusters and galaxies observed at low and moderate resolution.

M. C. expresses his gratitude to D. Sciama and A. Treves for continuous support and guidance during his Ph.D. work, and to R. L. Kurucz and B. Bell for hospitality and advice during his visit to the Harvard-Smithsonian Center for Astrophysics. Many helpful discussions with A. Buzzoni and G. Worthey are acknowledged. Partial support from MURST 40%-60% and from CNR bilateral grants is acknowledged.

APPENDIX

COMPUTATION OF INTEGRATED SPECTRAL INDICES

We illustrate in this appendix the role of synthetic "pseudocontinua" in the computation of integrated indices and the most significant advantage of using our grid instead of empirical fitting functions. As an example, the computation of the integrated index $\mathrm{Mg}_2^{\mathrm{tot}}$ is presented.

Recall the definition of the index for the ith single stellar component of a stellar population:

$$\mathrm{Mg}_2^i = -2.5 \log (F_f^i / F_c^i) , \tag{A1}$$

where F_f^i is the flux per unit wavelength in the Mg_2 central band (5154.125–5196.625 Å) and F_c^i is the "pseudocontinuum" flux per unit wavelength, computed by linear interpolation of the fluxes in the blue and red bands (4895.125–4957.625 Å and 5301.125–5366.125 Å, respectively).

In order to obtain the integrated index for a stellar population, all N contributions (F_f^i, F_c^i) must be summed:

$$\mathrm{Mg}_2^{\mathrm{tot}} = -2.5 \log \left(\sum_{i=1}^{N} w_i F_f^i \Big/ \sum_{i=1}^{N} F_c^i \right), \tag{A2}$$

where w_i represents the weight of the ith component according to the assumed luminosity function and population age.

The use of equation (A2), provided that the w_i are known from stellar evolution theories, is straightforward starting from our grid since the F_c^i are directly given and the F_f^i are easily derived in a completely consistent and homogeneous way from the listed indices, according to

$$F_f^i = F_c^i \, 10^{-0.4 \, \mathrm{Mg}_2^i} . \tag{A3}$$

On the contrary, $\mathrm{Mg}_2^{\mathrm{tot}}$ cannot be obtained by using empirical fitting functions alone since, like those given by WFGB94, they predict only individual Mg_2^i. In fact, equations (A2) and (A3) require, besides the individual Mg_2^i, the individual F_c^i also. A widely diffuse procedure for overcoming this problem is to approximate the F_c^i with interpolated values from theoretical flux libraries (see, e.g., Worthey 1994). Unfortunately, this procedure of mixing empirical and theoretical data may introduce unpredictable uncertainties due to the lack of internal consistency and homogeneity.

REFERENCES

Anders, E., & Grevesse, N. 1989, Geochim. Cosmochim. Acta, 53, 197
Barbuy, B. 1989, Ap&SS, 157, 111
———. 1994, ApJ, 430, 218
Bell, R. A., & Gustafsson, B. 1978, A&AS, 34, 229
———. 1989, MNRAS, 268, 771
Borges, A. C., Idiart, T. P., de Freitas Pacheco, J. A., & Thévenin, F. 1995, AJ, 110, 2408
Buzzoni, A., Gariboldi, G., & Mantegazza, L. 1992, AJ, 103, 1814
Buzzoni, A., Mantegazza, L., & Gariboldi, G. 1994, AJ, 107, 513
Chavez, M. 1995, Ph.D. thesis, Int. School for Adv. Stud. (SISSA/ISAS), Trieste
Chavez, M., Malagnini, M. L., & Morossi, C. 1995, ApJ, 440, 210
Faber, S. M., Friel, E. D., Burstein, D., & Gaskell, C. M. 1985, ApJS, 57, 711
Gorgas, J., Faber, S. M., Burstein, D., Gonzalez, J. J., Courteau, S., & Prosser, C. 1993, ApJS, 86, 157
Gulati, R. K., Malagnini, M. L., & Morossi, C. 1991, A&A, 247, 447
———. 1993, ApJ, 413, 166
Gustafsson, B., & Bell, R. A. 1979, A&A, 74, 313
Gustafsson, B., Bell, R. A., Eriksson, K., & Nordlund, A. 1975, A&A, 42, 407
Gustafsson, B., & Jørgensen, U. G. 1994, A&A Rev., 6, 16
Leitherer, C., Fritze-von Alvensleben, U., & Huchra, J., eds. 1996, ASP Conf. Proc. 98, From Stars to Galaxies (San Francisco: ASP)
Kraft, R. P. 1994, PASP, 106, 553
Kurucz, R. L. 1991, Rev. Mexicana Astron. Astrofis., 23, 187
———. 1993a, CD-ROM 13, ATLAS9 Stellar Atmospheres Programs and 2 km/s Grid (Cambridge: Smithsonian Astrophys. Obs.)

Kurucz, R. L. 1993b, CD-ROM 18, SYNTHE Spectrum Synthesis Programs and Line Data (Cambridge: Smithsonian Astrophys. Obs.)
———. 1993c, CD-ROM 19, Solar Abundance Model Atmospheres for 0, 1, 2, 4, 8 km/s (Cambridge: Smithsonian Astrophys. Obs.)
———. 1995, CfA preprint No. 4080
McQuitty, R. J., Jaffe, T. R., Friel, E. D., & Dalle Ore, C. M. 1994, AJ, 107, 359
Mould, J. 1978, ApJ, 220, 434
Pagel, B. E. J. 1996, in ASP Conf. Proc. 99, Cosmic Abundances, ed. S. E. Holt & G. Sonneborn (San Francisco: ASP), in press
Peterson, R., Dalle Ore, C. M., & Kurucz, R. L. 1993, ApJ, 404, 333
STSDAS. 1993, Space Telescope Science Data Analysis System, version 1.3.1 (Baltimore: STScI)
Thévenin, F. 1989, A&AS, 77, 137
Tripicco, M. J., & Bell, R. A. 1995, AJ, 110, 3035
Worthey, G. 1992, Ph.D. thesis, Univ. California, Santa Cruz
———. 1994, ApJS, 95, 107
Worthey, G., Faber, S. M., Gonzalez, J. J., & Burstein, D. 1994, ApJS, 94, 687 (WFGB94)